

Ferrofluids for Active Shock Absorbers

M D Rao^{1,3}, P S Goyal², Biswajit Panda² and R I K Moorthy¹

¹Department of Mechanical Engineering, Pillai College of Engineering, New Panvel, Navi Mumbai - 410206, India

²Department of Applied Sciences, Pillai College of Engineering, New Panvel, Navi Mumbai - 410206, India

Email: mdurgarao@mes.ac.in

Abstract. This paper deals with synthesis and characterization of a ferrofluid and examining its suitability for developing a damper whose damping behavior can be controlled by applying magnetic field. In particular, ferrofluids, consisting of oleic acid coated Fe₃O₄ nanoparticles dispersed in kerosene, have been synthesized and characterized. Oleic acid coated nanoparticles of Fe₃O₄ have been characterized using XRD, TEM and FTIR. These studies show that sizes of particles are in range of 6 to 17 nm and oleic acid is adsorbed on the surface of above particles. The role of damping medium on the damping behavior of a damper has been studied by carrying out studies with several different liquids. The effect of magnetic field on the damping behavior of ferrofluid based damper has also been studied. It is seen that damping ratio depends on the viscosity of damping medium. In particular, it is seen that damping ratio of a ferrofluid based damper increases on application of magnetic field. However, the sensitivity of damping ratio to the magnetic field has been found to be different for different ferrofluids. It seems, magnetic moment or size of the particle plays an important role in deciding the sensitivity of the damper. No attempt has been made to improve the sensitivity of the damper by optimizing various parameters. All the same, present studies provide a proof of concept for smart shock absorber.

1. Introduction

Cars and buses are fitted with suitable shock absorbers so that passengers do not experience bumpy and noisy ride [1]. Shock absorber is a device that controls unwanted oscillatory motion through a process known as damping. Currently available shock absorbers make use of ordinary fluids as damping medium and their damping behavior is decided at the design stage. However, it is of interest to have shock absorbers whose damping behavior could be controlled as per functional requirements. Ideally, one would like to have “*Smart Shock Absorber*”, whose damping properties could be controlled by application of suitable electric or magnetic fields. Magnetorheological Dampers [2-4], which use magnetorheological (MR) fluids as the damping medium, have above characteristics but they have not been commercially successful. MR fluids consist of a suspension of large size (~ 10 μm) magnetic particles and these particles aggregate and settle down over a period of time. That is, MR fluids are not stable and their rheological properties change with time. It is felt that for an active damper or shock absorber [5-8], one should use ferrofluid instead of MR fluid as the damping medium.

³ To whom any correspondence should be addressed.



Ferrofluids are better suited for this purpose. They are stable as sizes of magnetic particles (~ 50 nm) in ferrofluids are much smaller than those in MR fluids [9-11]. It is known that viscosity of ferrofluids also varies with magnetic field [12]. This paper deals with synthesis and characterization of ferrofluids and studying the damping behavior of ferrofluid based damper, both, with and without magnetic field.

Ferrofluid (also referred to as magnetic liquid) is a unique material that has both the liquid and magnetic properties [9,10]. They are colloidal suspensions of magnetic nano-particles (size ~ 10 nm) in a liquid medium. To avoid coagulation of magnetic particles, they are coated with suitable surfactant molecules. The ferrofluid used in present studies was synthesized in our laboratory [13]. It consists of oleic acid coated nanoparticles of magnetite, Fe_3O_4 , dispersed in carrier liquid kerosene. The damping behavior of a damper having above ferrofluid as the damping medium, has been studied. The effect of magnetic field on the damping behavior of above damper has also been examined.

The next section gives the details of synthesis and characterization of ferrofluid. Section 3 gives the experimental details of the set-up used for studying the damping behavior of the damper. Results of above studies for several different experimental conditions are given in section 4. In the end, section 5 gives a summary.

2. Synthesis and Characterization of Ferrofluid

The synthesis of ferrofluid involves preparing of nanoparticles, coating them with surfactant molecules and dispersing these particles in suitable carrier liquid [9-11]. We have synthesized ferrofluids using oleic acid coated Fe_3O_4 nanoparticles, which were dispersed in kerosene. Nanoparticles of Fe_3O_4 were synthesized using wet chemical route, which involves co-precipitation of Fe^{2+} and Fe^{3+} in alkali solution. The details of this method of preparing nanoparticles of Fe_3O_4 and coating them with oleic are given in a review paper by Mehta and Upadhyay [9]. We have synthesized two categories of ferrofluids. In case of Category-I, Fe_3O_4 was prepared by reacting ferric chloride (FeCl_3) with ferrous sulfate (FeSO_4) in an aqueous medium. In case of Category-II, the starting salt for preparing Fe_3O_4 was ferric chloride (FeCl_3) and the required ferrous chloride (FeCl_2) was obtained by reduction of FeCl_3 . The pH of the aqueous solution was controlled using ammonia solution. The Iron (III) chloride (FeCl_3), ferrous (II) sulfate (FeSO_4), oleic acid and 25% ammonia solution used for above studies, were purchased from Sigma-Aldrich, USA. All chemicals were of analytical grade and were used as received. The full details of method of synthesis and characterization of magnetic nanoparticles are given in our earlier paper [13].

The above samples have been characterized using X-ray diffraction (XRD), Transmission electron microscopy (TEM), and Fourier Transform Infra-red (FTIR) spectroscopy. XRD studies provided information about the structure and the composition of the constituents of the nanoparticles. The sizes of above nanoparticles were obtained using TEM. FTIR studies provided information on nature and extent of binding of oleic acid on particle surface. The salient features of these studies for Category-I (FeSO_4 based samples) are given below [13].

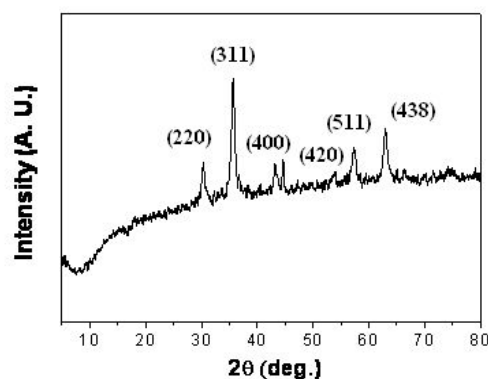


Figure 1. X-ray Diffraction pattern obtained from the magnetic nanoparticles.

Figure 1 shows the XRD pattern obtained from the magnetic nanoparticles. The existence of sharp Bragg peaks suggests that nanoparticles are crystalline in nature. The position of peaks correspond to single phase cubic structure of Fe_3O_4 with a lattice constant $a = 8.325 \text{ \AA}$, which is in very good agreement with published data [14]. It is noted that there is broadening of the Bragg peaks and this arises because of finite sizes of the particles. The particle size as obtained from the width (β) of (311) Bragg peak using Debye–Scherrer equation ($R = 0.9\lambda/(\beta \cos \theta)$) is about 12.6 nm.

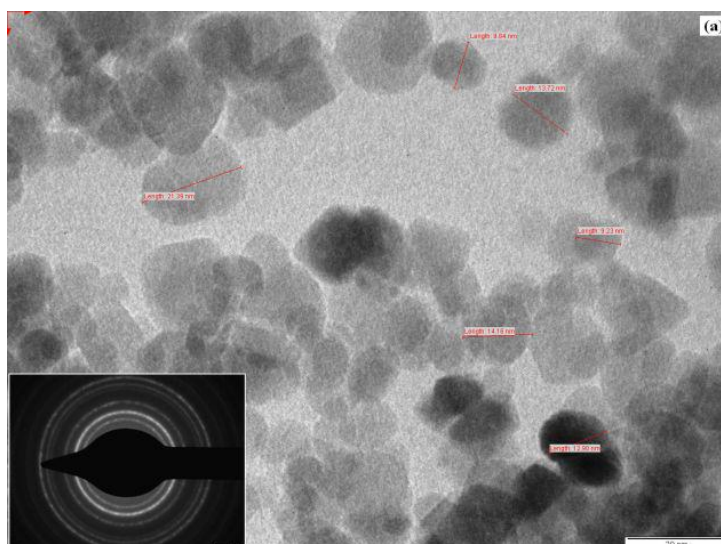


Figure 2. TEM micrograph of Fe_3O_4 nanoparticles.

Figure 2 shows the TEM micrograph of Fe_3O_4 nanoparticles. It is seen that most of the nanoparticles are spheres of varying sizes.

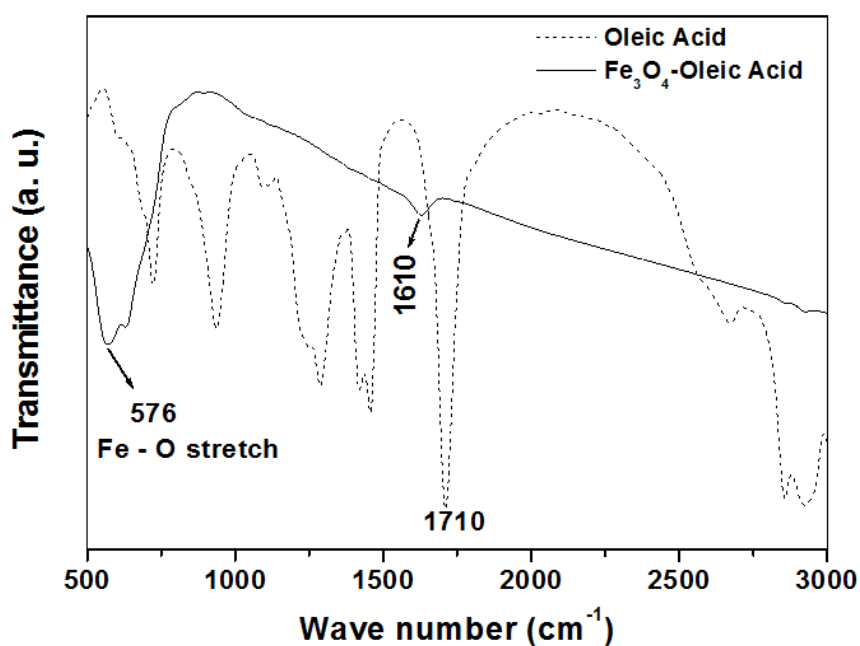


Figure 3. FTIR Spectra for pure oleic acid and for oleic acid coated Fe_3O_4 nanoparticles.

Figure 3 shows the comparison of FTIR spectra for pure oleic acid and those for oleic acid coated Fe_3O_4 nanoparticles. It is seen that the absorption bands for the pure oleic acid are well resolved, but those of the Fe_3O_4 – oleic acid are rather broad and few. The relevant peaks are in region of $1500\text{--}1750\text{ cm}^{-1}$. C = O vibration from –COOH group of oleic acid gives a peak at 1710 cm^{-1} for pure oleic acid. This peak shifts to 1589 cm^{-1} , when oleic acid is adsorbed on Fe_3O_4 particles. The absence of 1710 cm^{-1} peak in spectra of oleic acid coated nanoparticles suggests that most of the oleic acid in nanoparticle system is adsorbed on Fe_3O_4 nanoparticles. The IR band observed at around 576 cm^{-1} can be ascribed to the Fe–O stretching vibrational mode of Fe_3O_4 nanoparticles [15].

3. Experimental set-up for studying damping behavior of the damper

Figure 4 is a schematic drawing of the experimental set-up that has been used for studying the damping behavior of the damper. The vibrating system is comprised of a beam pivoted at its end and supported by a helical spring at its other end.

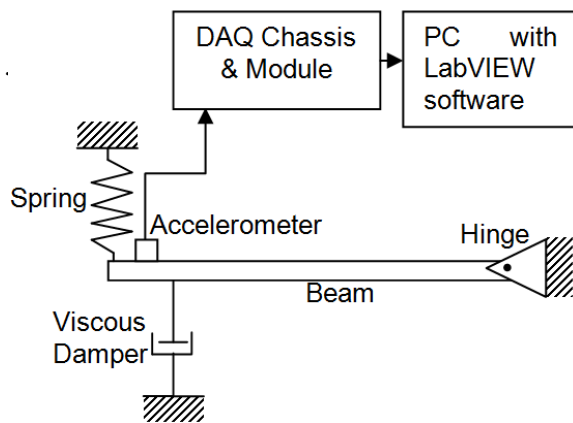


Figure 4. Schematic drawing of the set-up used for measuring damping ratio of a damper

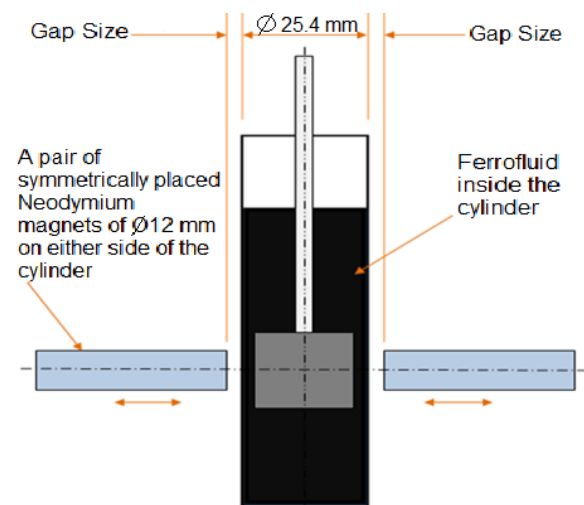
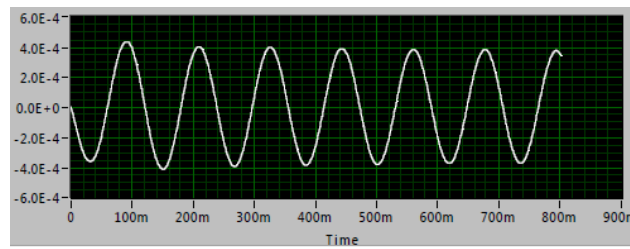


Figure 5. Viscous damper along with the magnets.

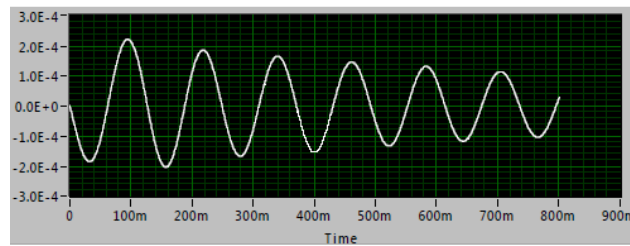
The beam is set in free vibration mode by using a small initial angular displacement. Vibrations are sensed by a uni-axial accelerometer which is connected to a suitable data acquisition module (DAQ) through a data cable. The DAQ module is connected to a personal computer in which the National Instruments' LabVIEW programming software (version 12) is installed. The experiment involved measurement of acceleration versus time graphs using the accelerometer for sensing and LabVIEW software for gathering and analyzing the data. Displacement versus time data was obtained by integrating the acceleration data twice. To study the damping behavior of the viscous damper, the damper containing damping fluid is connected at a suitable distance from the spring as shown in figure 4. A piston and cylinder mechanism of the viscous damper is shown in figure 5 with a suitable fluid. It is possible to change the damping fluid of the damper and apply suitable magnetic field to the damping medium using neodymium magnets. The magnetic field can be varied by moving the neodymium magnets (i.e. by varying the gap size) as shown in the figure.

Damping medium slows down and reduces the amplitude of vibratory motion of the piston. The damping ratio ζ is extracted from the displacement versus time plots. It is known that if x_n is the amplitude at the end of n^{th} cycle, then logarithmic decrement δ is given by:

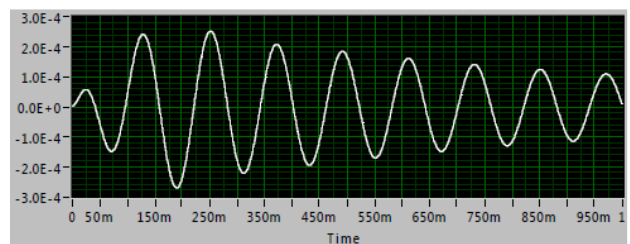
$$\delta = \ln \left(\frac{x_1}{x_{n+1}} \right) \quad (1)$$



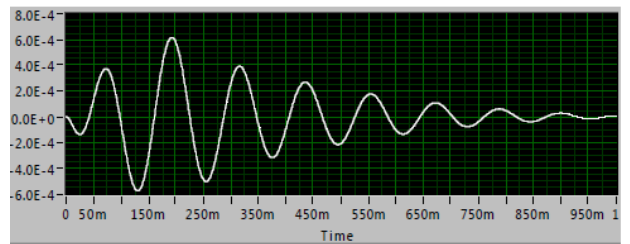
(a) Undamped (no damper connected)



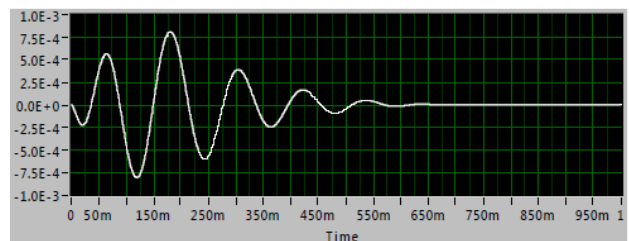
(b) Damper (with water as damping medium)



(c) Ferrofluid (FF-Cl₂-II) based damper without magnetic field ($H = 0$ kG)



(d) Ferrofluid (FF-Cl₂-II) based damper with magnetic field ($H = 3.2$ kG)



(e) Ferrofluid (FF-Cl₂-II) based damper with magnetic field ($H = 4.5$ kG)

Figure 6. Displacement versus Time graphs for viscous damper under different experimental conditions.

The damping ratio ζ is given by:

$$\zeta = \sqrt{\frac{\delta^2}{\delta^2 + 4\pi^2}} \quad (2)$$

We have used the set-up for measuring ζ for several different damping media, namely, viscous liquids (CTAB/ NaSal system) [16] and three different ferrofluids. The effect of magnetic field on ζ has been examined for ferrofluid based dampers. Typical measured displacement-time graphs are shown in figure 6. Because of integration errors, the first two cycles in the figures have not been considered for computing logarithmic decrement δ .

4. Results and Discussions

4.1. Effect of liquid viscosity on damping ratio

The effect of viscosity (η) of the damping fluid on the damping ratio ζ of the damper has been studied using solution of Cetyltrimethylammonium Bromide (CTAB) and Sodium Salicylate (NaSal) as the damping medium. The viscosity of (CTAB + NaSal) solution depends on the relative concentrations of CTAB and NaSal [16] and thus these studies provided information on the variation of damping ratio ζ with the viscosity of the damping fluid. Measurements have been made for (0.1M CTAB + x NaSal) for x = 0.0, 0.02, 0.05 and 0.08 M. The viscosities of these solutions are 1.5 cP, 30 cP, 50 cP and 100 cP respectively. The measurements were also made for a damper having water ($\eta = 1.0$) as the damping fluid. For sake of completeness measurements were also made on an un-damped damper (free vibrations). Results are shown in table 1 and figure 7. As expected, from figure 6, it is seen that the damping ratio increases with increase in the viscosity of damping medium.

Table 1. Effect of viscosity of damping medium on the damping ratio (ζ) of damper.

Damping Medium	Viscosity	$\zeta \times 10^{-3}$
Undamped	-	2.3
Water	1	10.9
0.1M CTAB + 0.0M NaSal	1.5	14.9
0.1M CTAB + 0.02M NaSal	30	123.6
0.1M CTAB + 0.05M NaSal	50	170.4
0.1M CTAB + 0.08M NaSal	100	532.8

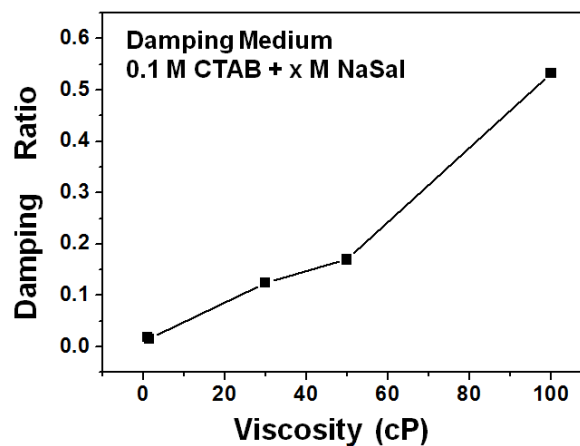


Figure 7. Displacement Damping Ratio vs. Viscosity for (0.1M CTAB + x M NaSal) solutions as damping fluid for x = 0.0, 0.02, 0.05 and 0.08 M.

4.2. Ferrofluid based dampers: Effect of magnetic field on damping ratio

The damping behavior of ferrofluid based dampers was studied for following three sets of ferrofluids:

(a) Ferrofluids (Category-I) where Fe_3O_4 was prepared using FeCl_3 and FeSO_4 . Measurements were made corresponding to two batches, referred to as FF-SO₄-I and FF-SO₄-II.

(b) Ferrofluids (Category-II) where Fe_3O_4 was prepared using FeCl_3 and FeCl_2 . Measurements were made corresponding to two batches, referred to as FF-Cl₂-I and FF-Cl₂-II.

(c) Commercially obtained oil based ferrofluid whose composition was not known (referred to as FF-Comm.)

The damping ratio ζ was measured for above samples, both, with and without magnetic field. Measurements were made for magnetic field (H) in the range of 0.0 to 4.5 kG. The magnetic field at piston-cylinder interface was measured using Hall-effect based sensor coupled to a gaussmeter. The results of the above studies are shown in figure 8. It is clear that damping ratio increases with magnetic field for all the ferrofluids. However, the rate of increase of ζ for a given increase in field is different for different ferrofluids. That is, sensitivity of ζ to the magnetic field is not same for all ferrofluids. This is not surprising as zero-field viscosity and particle sizes are expected to be different for different ferrofluids. To get an idea of comparative sensitivities of different ferrofluids, table 2 compares the increase in values of ζ when a fixed field of 4.5 kG is applied to all the five ferrofluids.

Table 2. Variation of damping ratio (ζ) with magnetic field for different ferrofluids, for a ferrofluid based damper.

Damping Medium	Damping Ratio ζ (for H = 0.0 kG)	Damping Ratio ζ_F (for H = 4.5 kG)	ζ_F/ζ (%)
FF-Comm.	0.072	0.085	18
FF-SO ₄ -I	0.019	0.035	84
FF-SO ₄ -II	0.023	0.029	26
FF-Cl ₂ -I	0.017	0.066	388
FF-Cl ₂ -II	0.020	0.148	740

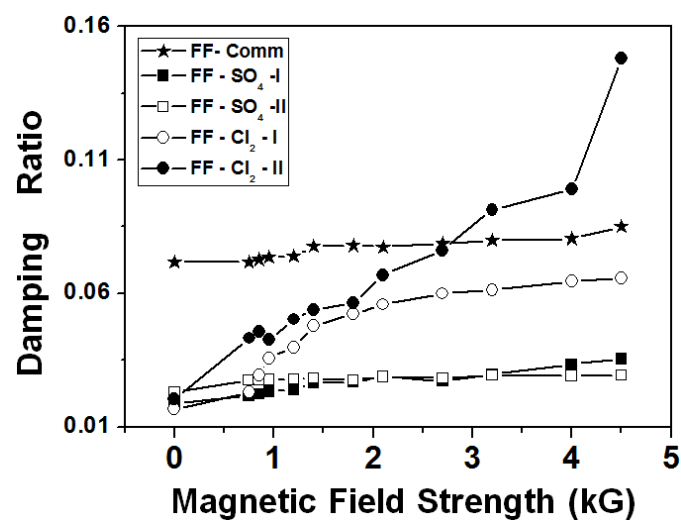


Figure 8. Variation of damping ratio with magnetic field for different ferrofluids.

Table 2 and figure 8 show that zero-field damping ratio (~ 0.02) is nearly same for all indigenously synthesized ferrofluids. However, this value is much larger (~ 0.07) for commercial fluid. This may be attributed to the fact that viscosity of commercial ferrofluid is more (perhaps because of larger particle concentration and viscous carrier liquid) as compared to that for indigenously synthesized ferrofluids. It is interesting to note that sensitivity of damper using category-II ferrofluid (Fe_3O_4 prepared using $\text{FeCl}_3/\text{FeCl}_2$) is much better compared to the one that uses category – I ferrofluids (Fe_3O_4 prepared using $\text{FeCl}_3/\text{FeSO}_4$) or the one that uses commercial ferrofluid. For example, when magnetic field is increased from 0.0 kG to 4.5 kG, the damping ratio for the former category of dampers increases by about 500% and that for the latter category, increases by about 50%. No effort has been made to understand the reasons for the above. It is known that magnetic nanoparticles form chains in presence of magnetic field and that gives rise to increase in viscosity and the damping ratio. The chains would be more rigid and the damping ratio would be higher if particle size or its magnetic moment is large [17]. It is likely that particle sizes are different in different ferrofluids. The results of such detailed studies will be published in a future paper.

5. Summary

The shock absorbers used in cars and buses make use of ordinary fluids as damping medium and their damping behavior is decided at the design stage. In practice, one needs a shock absorber whose damping could be changed depending on the road condition or the load. It is thus of interest to have “*Smart Shock Absorber*” whose damping properties could be controlled by application of suitable electric or magnetic fields. This paper deals with development of a damper that uses ferrofluid as the damping medium. It is shown that damping ratio of above damper can be varied by applying magnetic field to the damping medium. The effect of magnetic field on damping ratio has been studied using several different ferrofluids.

Ferrofluids, required for above studies, have been synthesized and characterized indigenously. They consist of oleic acid coated nano-particles of magnetite (Fe_3O_4), dispersed in kerosene. Fe_3O_4 is prepared by using two different chemical routes ($\text{FeSO}_4/\text{FeCl}_3$ and $\text{FeCl}_2/\text{FeCl}_3$). Nano-particles of Fe_3O_4 prepared by using $\text{FeSO}_4/\text{FeCl}_3$ were characterized using XRD, TEM and FTIR. It was seen that sizes of magnetic particles are in 6 to 17 nm range, with a dominant population at 12-14 nm.

The damping ratio of a piston-cylinder type damper has been measured using several different damping mediums, such as viscous liquids, commercial ferrofluid and indigenously synthesized ferrofluids. It was seen that there is a direct correlation between the viscosity of the damping medium and the damping ratio. In case of ferrofluid based dampers, it was seen that damping ratio increases with magnetic field. The sensitivity or the rate of increase of damping ratio with magnetic field was, however, found to be different for different ferrofluids. No attempt has been made to understand the reasons for the above. It seems the sensitivity of the damper depends on sizes and concentrations of nanoparticles in the ferrofluid.

The above studies provide a technological demonstration of ferrofluid based active shock absorber. It is, however, important to quantify the role of various parameters on the damping behavior before one designs and manufactures the *Active Shock Absorber* for use in a vehicle.

Acknowledgments

We thank Priam Pillai for encouragement and useful discussions. This research is financially supported by All India Council of Technical Education (AICTE)—New Delhi, under Research Proposal Scheme 8023/RID/RPS-93(Pvt)/2011-12.

6. References

- [1] Dixon J C 2007 *The Shock Absorber Handbook* 2nd Edition John Wiley and Sons
- [2] Sapinski B 2009 *Mechanics* **28** 18
- [3] Kumbhar B K, Patil S R and Sawant S M 2015 *Engineering Science and Technology, an International Journal* **18** 432
- [4] Zhu X, Jing X and Li Cheng 2015 *J. Intelligent Material Systems and Structures* **26** 881
- [5] Raj K and Moskowitz R 1980 *IEEE Transactions on Magnetics* **16** 358
- [6] Nakatsuka K, Yokoyama H and Shimoiizaka J 1987 *J. Mag. Mat.* **65** 359

- [7] Bashtovoi V G, Kabachnikov D N and Kolobov A Y 2002 *J. Mag. Mag. Mat.* **252** 312
- [8] Yang W, Li D and Feng Z 2013 *J. Vibrations and Controls* **19** 183
- [9] Mehta R V and Upadhyay R V 1999 *Current Science* **76** 305
- [10] Odenbach S 2002 *Ferrofluids: Magnetically controlled ferrofluids and their applications* (Ed) Springer Verlag Berlin
- [11] Charles S *The preparation of magnetic fluids* 3-18 in [10]
- [12] Patel R, Upadhyay R V and Mehta R V 2003 *J. Coll. Int. Sci.* **263** 661
- [13] Panda Biswajit and Goyal P S 2015 *AIP Conference Proceedings* **1665** 050020
- [14] Lan Qiang, Liu Chao, Yang Fei, Liu Shangying, Xu Jian and Sun Dejun 2007 *J. Coll. Int. Sci.* **310** 260
- [15] Nigam Saumya, Barick K C, Bahadur D 2011 *J. Mag. Mag. Mat.* **323** 237
- [16] Aswal V K, Goyal P S and Thiyagarajan R 1998 *J. Phys.Chem.B* **102** 2469
- [17] Butter K, Bomans P H H, Frederik P M, Vroege G J and Philipse A P 2003 *Nature Materials* **2** 88